iScience

CellPress
OPEN ACCESS

Article

Closantel is an allosteric inhibitor of human Taspase1

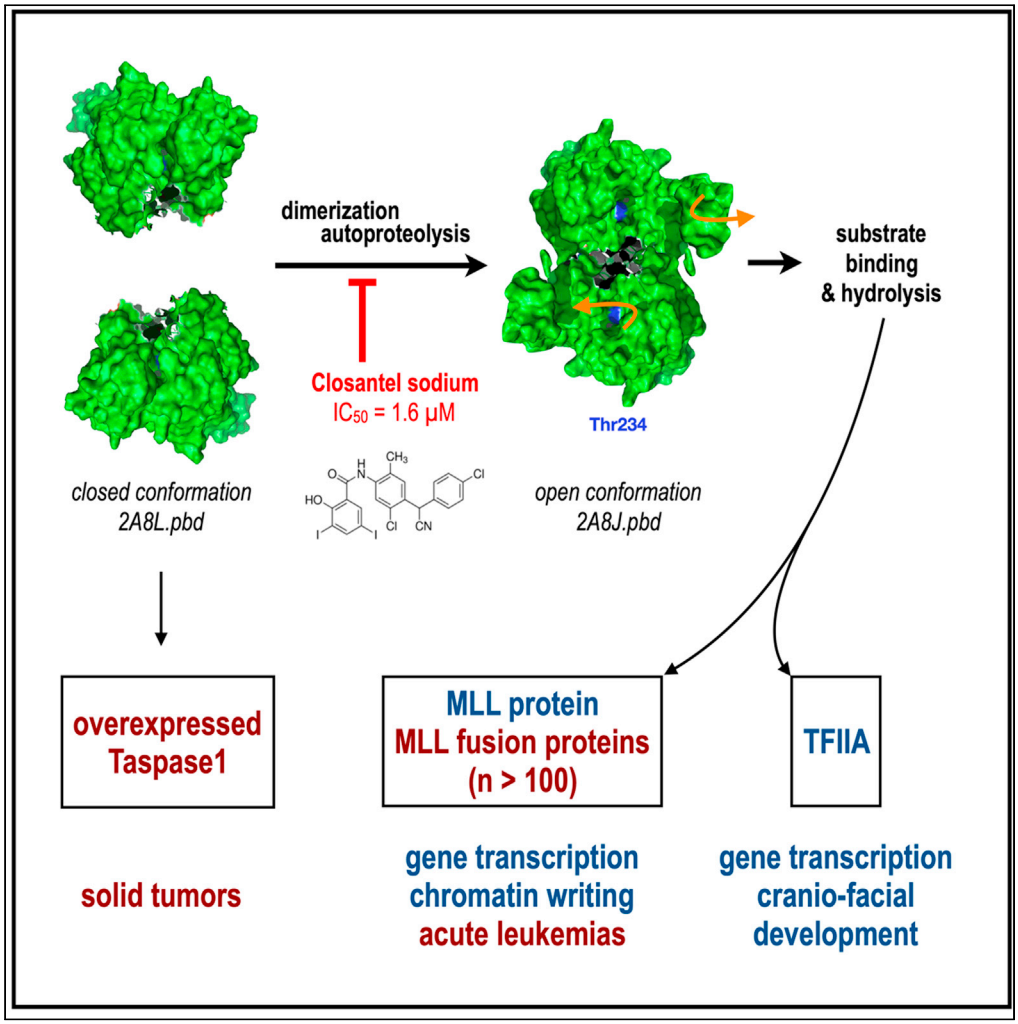

Vanessa Luciano, Ewgenij Proschak, Julian D. Langer, Stefan Knapp, Jan Heering, Rolf Marschalek

rolf.marschalek@em.uni-frankfurt.de

Highlights

Taspase1 hydrolyzes members of the Trithorax family and TFIIA•

Taspase1 acts in a stoichiometric fashion, performing only a single cleavage reaction•

HTFR assay allowed the identification of an allosteric inhibitor•

The inhibitor can be used for target validation and as a lead substance for drug design

Luciano et al., iScience 24, 103524
December 17, 2021
https://doi.org/10.1016/j.isci.2021.103524

iScience

CellPress
OPEN ACCESS

Article

Closantel is an allosteric inhibitor of human Taspase1

Vanessa Luciano,[1] Ewgenij Proschak,[2] Julian D. Langer,[3] Stefan Knapp,[2] Jan Heering,[4,5] and Rolf Marschalek[1,5,6,*]

SUMMARY

Dimerization of Taspase1 activates an intrinsic serine protease function that leads to the catalytic Thr234 residue, which allows to catalyze the consensus sequence $Q^{-3}X^{-2}D^{-1}\cdot G^{1}X^{2}D^{3}D^{4}$, present in Trithorax family members and TFIIA. Noteworthy, Taspase1 performs only a single hydrolytic step on substrate proteins, which makes it impossible to screen for inhibitors in a classical screening approach. Here, we report the development of an HTRF reporter assay that allowed the identification of an inhibitor, Closantel sodium, that inhibits Taspase1 in a noncovalent fashion (IC_{50} = 1.6 μM). The novel inhibitor interferes with the dimerization step and/or the intrinsic serine protease function of the proenzyme. Of interest, Taspase1 is required to activate the oncogenic functions of the leukemogenic AF4-MLL fusion protein and was shown in several studies to be overexpressed in many solid tumors. Therefore, the inhibitor may be useful for further validation of Taspase1 as a target for cancer therapy.

INTRODUCTION

Taspase1, an evolutionarily highly conserved threonine protease (type 2 asparaginase—a subfamily of N-terminal nucleophile (Ntn) hydrolases; Brannigan et al., 1995; Oinonen et al., 2000), has been identified as an MLL-specific protease that recognizes two heptapeptide recognition sequences, CS1 (QVD•GADD) and CS2 (QLD•GVDD), within the MLL (mixed-lineage leukemia) protein sequences and causes hydrolysis at 2,666/2,667 and 2,718/2,719 within *H. sapiens* MLL to generate the $p320^{N}$ and $p180^{C}$ protein fragments (Hsieh et al., 2003a, 2003b). Consequently, the resulting MLL protein fragments ($p320^{N}$ and $p180^{C}$) form a high-molecular-weight complex via the FYRN and FYRC domains (Pless et al., 2011). The resulting MLL multi-protein complex carries out important epigenetic functions ($H3K4_{me3}$; $H4K16_{Ac}$; H_{Ac}) that are directly linked to transcriptional maintenance (Nakamura et al., 2002; Dou et al., 2005). Of importance, a crystal structure of Taspase1 has been published soon after the discovery of this protein (Khan et al., 2005), which facilitates the study of this unusual protease at the molecular level. The Taspase1 structure has been refined and investigated in a more recent study (Nagaratnam et al., 2021). This study has provided new structural information, as well as revealed the functional importance of a long alpha-helix at the C-terminal portion of the α-subunit for the catalytic activity of the β-subunit of Taspase1.

Besides its role in the functional processing of MLL protein, Taspase1 also plays an important role in TFIIA processing (Zhou et al., 2006; Malecová et al., 2015), and this function appears to be quite important for fetal hematopoiesis and proper facial and axial skeleton development (Niizuma et al., 2021). In particular, cranial development and craniofacial anomalies have been linked to a specific V343M mutation in Taspase1 (Takeda et al., 2015; Balkin et al., 2019).

Proper cleavage of MLL has been associated with cell-cycle control and apoptosis (Takeda et al., 2006; Chen et al., 2010) and the regulation of gene transcription via the MLL/COMPASS complex (Zhao et al., 2019). The latter work investigated the steady-state MLL protein abundance in the presence or absence of Taspase1, demonstrating that Taspase1-mediated cleavage of MLL leads to a higher turnover of the MLL protein complex.

Several other studies have linked Taspase1 overexpression to cancer progression and metastasis, for instance in breast cancer (Dong et al., 2014), head and neck cancer (Gribko et al., 2017), and gall bladder

[1]Institute of Pharmaceutical Biology/DCAL, Goethe-University of Frankfurt, Biocenter, Max-von-Laue-Street 9, 60438 Frankfurt/Main, Germany

[2]Institute of Pharmaceutical Chemistry, Goethe-University of Frankfurt, Biocenter, Max-von-Laue-Street 9, 60438 Frankfurt/Main, Germany

[3]MPI for Biophysics, Max-von-Laue-Street 3, 60438 Frankfurt/Main, Germany

[4]Fraunhofer Institute for Translational Medicine and Pharmacology ITMP, Theodor-Stern-Kai 7, 60596 Frankfurt/Main, Germany

[5]These authors contributed equally

[6]Lead contact

*Correspondence: rolf.marschalek@em.uni-frankfurt.de

https://doi.org/10.1016/j.isci.2021.103524

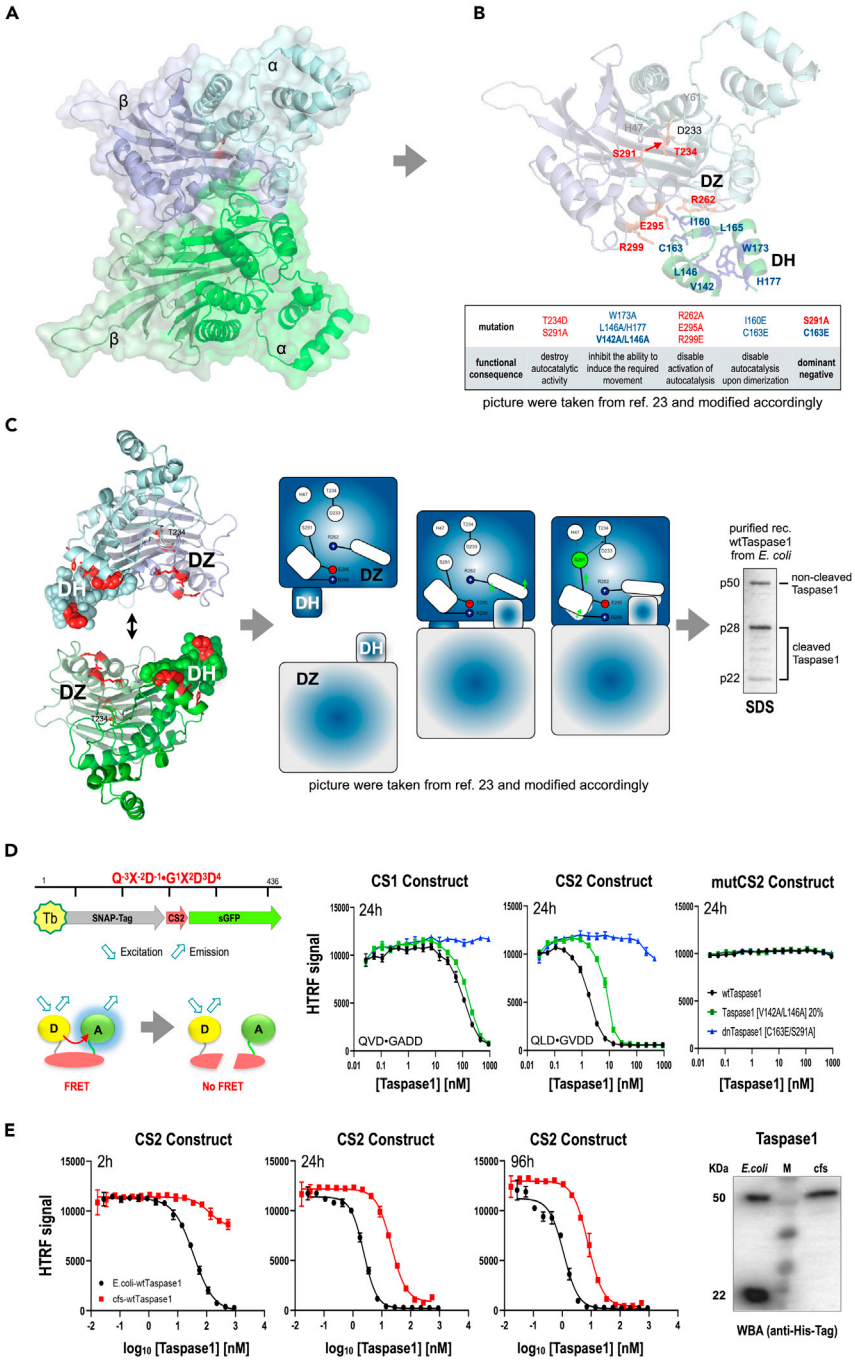

Figure 1. Molecular function of Taspase1 and setting up the HTRF assay

(A) Molecular modeling of the Taspase1 homodimer with its α and β subunits (20).

(B) Model of a single monomer of Taspase1 with the docking head of the second subunit (amino acids 140–180) and the critical amino acids that are all necessary to explain the intrinsic serine protease function (D233, T234, R262, S291, E295, and R299).

(C) During the dimerization process, the two docking heads bind to the docking zone of the opposing Taspase1 monomer, respectively. The scheme in the middle explains the steps that lead to the positioning of the serine residue next to the D233/T234 peptide bond. On the right: Taspase1 isolated from *E. coli*, demonstrating that more than half of the Taspase1 molecules are already hydrolyzed into P28 and p22 (as visualized on Coomassie-stained SDS page).

(D) Substrate protein. The SNAP-tag is labeled with Terbium cryptate (Tb-SNAP) that serves as the FRET donor. Superfolder GFP (sGFP) is utilized as FRET acceptor. Tb-SNAP and sGFP are linked to each other by the cleavage sites

Figure 1. *Continued*

from the MLL protein (consensus sequence is indicated). FRET occurs with high efficiency when the substrate is not hydrolyzed. Cleavage causes separation of SNAP and sGFP, which results in drastic reduction of FRET. The reduction of sGFP fluorescence translates into HTRF being almost zero when being recorded on completely hydrolyzed substrate. Right panels: hydrolysis of the substrate protein with MLL CS1 and CS2, respectively. The cleavage site sequences are indicated. Three different Taspases were used: wild-type Taspase1, Taspase1 with V142A/L1476A that has about 20% catalytic activity, as well as dnTASP1 (C163E, S291A). 1 nM of CS1 or CS2 substrate protein were incubated for 24 h with Taspase1 variants at concentrations ranging from 0.027 nM to 900 nM (16 serial dilutions), respectively. Data are the mean ± SD; n = 3.

(E) *E. coli*-produced already auto-activated Taspase1 (black) is compared with freshly cell-free-produced (cfs) Taspase1 (both wild type). Cleavage of CS2 was detected by HTRF after 2, 24, and 96 h. Data are the mean ± SD; n = 3. $R^2 = 0.82$ for cfs after 2 h. For all over curves R^2 was ≥0.98. This comparison revealed an augmented window for screening of potential inhibitors when using 30 nM cfs-Taspase1 and detection after 24 h. On the right: western blot experiment performed with *E. coli*- and cfs-Taspase1, indicating that cfs-Taspase1 is not yet auto-activated and hence fully suitable for screening of inhibitors with potentially different modes of inhibition.

cancer (Zhang et al., 2020), just to mention a few. In *MLL*-r leukemia, all reciprocal fusion proteins are subject to Taspase1 cleavage (Marschalek, 2020). In particular, the AF4-MLL fusion protein requires Taspase1 for its steady-state stability. Unprocessed AF4-MLL is rapidly degraded via SIAH1/2, two E3-ligases involved in the control of protein abundance of AF4 (Bursen et al., 2004), whereas Taspase1 processed AF4-MLL assembles into a very stable high-molecular-weight complex (half-life of ∼96 h). However, overexpression of Taspase1 alone or in combination with known oncoproteins does not cause malignant transformation, indicating that Taspase1 has different functions and drives a large variety of changes in the cellular proteome, classifying Taspase1 as a "non-oncogene addicted" protease (Chen et al., 2010).

We had previously already dissected several functions of Taspase1 by site-directed mutagenesis, and we have analyzed the consequences of the generated mutants. This has led to a clear picture of how Taspase1 is activated to function as a specific protease for its target proteins. It was also discovered that Taspase1 is not a classical enzyme and that it is able to bind to several substrate proteins. Our model suggests that Taspase1 becomes activated by dimerization, which subsequently allows a single hydrolysis of any substrate protein (Sabiani et al., 2015). This particular property of Taspase1 also explains why no inhibitor has been identified so far. Although some authors have claimed so (Lee et al., 2009; Chen et al., 2012; van den Boom et al., 2014), no one has described a drug able to inhibit Taspase1 at physiologically relevant concentrations. Based on our mutation analysis (Sabiani et al., 2015) and the mechanism of activation, we proposed that allosteric inhibition would be promising. Thus a perfect drug should be able to block the initial steps to maintain Taspase1 in its inactive state. Following this strategy and by screening a Food and Drug Administration (FDA)-approved drug library, we were successful to identify a first Taspase1 inhibitor that works at low μM concentrations.

RESULTS

Functional characterization of Taspase1

As described recently (Sabiani et al., 2015), Taspase1 was *in silico* re-modelled from the available crystal structure (Khan et al., 2005; see Figure 1A). Subsequent mutagenesis studies at single amino acids (see Figure 1B) revealed the potential mechanism of Taspase1 activation (see Figure 1C). Briefly, when the Taspase1 docking head (DH: amino acids 140–180) made contact with the docking zone (DZ) of an opposing Taspase1 monomer, a slight movement of R262 toward E295 results in a movement of S291 toward the non-hydrolyzed D233•T234 peptide bond, which is then hydrolyzed by the serine protease activity of S291. Because this happens simultaneously in both Taspase1 monomers, the catalytically active $\alpha_2\beta_2$ hetero-tetrameric structure of Taspase1 is formed. The processing can be readily seen when preparing recombinant Taspase1 from *Escherichia coli* (see Figure 1C, right SDS page), where the p50 Taspase1 monomers became auto-hydrolyzed into the p28 α- and p22 β-subunits. The p22 subunits carry each a catalytically active N-terminal threonine residue (T234) that is necessary for the hydrolysis of target proteins.

Developing a homogeneous time resolved FRET reporter system for Taspase1 cleavage

Next, we developed a sensitive assay system that allowed us to monitor the cleavage of Taspase1 substrates in a time-resolved fashion. From our previous work (Sabiani et al., 2015) we had already identified some interesting Taspase1 mutants: a partially compromised Taspase1 that carried 2 mutated amino acids

in the docking head zone that made it less rigid (V142A, L146A: 20% activity) and a dominant-negative version of Taspase1 (dnTASP1; C163E, S291A: <<1% activity).

The reporter assay was based on an SNAP-Tag (for covalent labeling with Terbium cryptate), fused by one of the two different Taspase1 cleavage sites of MLL (CS1 or CS2) to super-folded GFP (sGFP; see Figure 1D, left). By using both substrate proteins, an assay based on homogeneous time-resolved FRET (HTRF) was established. The cleavage assay utilizes Terbium cryptate (Tb-cryp; Cisbio) as FRET donor, which forms an optimal FRET pair with the sGFP that serves as FRET acceptor (Riddle et al., 2006). Both donor and acceptor are part of the same fusion protein and separated only by the small segment encompassing the Taspase1 cleavage site. The close proximity enables very efficient FRET, which in turn allows sensitive HTRF readout even with very low concentrations of substrate protein (1 nM). After cleavage by Taspase1, Tb-cryp-labeled SNAP and sGFP separate from one another, which results in reduction in FRET. The fact that both FRET partners are $\geq$20 kDa in size in combination with the low concentration thereby reduces diffusion-enhanced FRET to a bare minimum. In effect the assay provides a good assay window. It can easily be conducted in 384 well format with only 20 μL final assay volume. The high fluorescence stability of Tb-cryp and sGFP allows for repeated HTRF measurements.

When using this technology with CS1 and CS2 reporter constructs, surprising results were obtained. As shown in Figure 1D (right panels; Taspase1 concentrations ranged between 0.027 nM and 900 nM), the cleavage rate of the CS1- and CS2-substrate proteins was quite different. Although Taspase1 readily hydrolyzed the CS2 cleavage site of MLL, CS1 was only poorly hydrolyzed. Therefore, the differences between wild type, the compromised double mutant (V142A, L146A), and the inactive version of Taspase1 (dnTasp1) can best be investigated on the CS2-reporter construct. CS1 cleavage was so inefficient that there was no difference observable between wild-type Taspase1 and compromised double mutant, whereas the dnTASP1 remained inactive on CS1. Therefore, we used the CS2-substrate for all subsequent experiments at a final concentration of 1 nM.

E. coli-produced wild-type Taspase1 (hereafter named "*E. coli*-Taspase1") is already partially activated once purification is accomplished. Therefore, we decided to establish a coupled *in vitro* transcription/translation system followed by rapid purification of cell-free synthesized wild-type Taspase1 (hereafter named "cfs-Taspase1"). With this strategy we were able to isolate Taspase1 that had not yet been activated by auto-proteolytic cleavage. This was demonstrated in a western blot experiment (shown on the right in Figure 1E) where the C-terminal His-tagged Taspase1 was either expressed in *E. coli*- or *in vitro* Taspase1. *E. coli*-Taspase1 revealed the typical p50 and p22 bands, whereas cfs-Taspase1 was still in its enzymatically inactive p50 form. The p28 fragment does not possess a His-tag and is hence not detected in the western blot. According to the molecular mechanism of coupled Taspase1 dimerization and auto-activation the purified cfs-Taspase1 is, hence, likely still monomeric when it is added to the activity assay.

As time is critical, all assays performed were done directly after the production of cfs-Taspase1. A first experiment is summarized in Figure 1E, where we tested cfs-Taspase1 against *E. coli*-Taspase1 (both wild-type) after 2 h, 24 h, and 96 h in the established HTRF reporter assay. *E. coli*-Taspase1 was active from the beginning of the experiment and cleaved CS2 in a time-dependent manner. For complete cleavage within 2 h about 900 nM Taspase1 was needed, which corresponds to a 900-fold molar excess of Taspase1 to CS2 substrate (1 nM). But a much lower concentration of *E. coli*-Taspase1, of about 10 nM, was capable of almost completely processing all CS2 within 24 h. Between 24 h and 96 h the concentration corresponding to ~50% CS2 cleavage did further slightly reduce by a factor of 2.

As expected, cleavage by cfs-Taspase1 lagged behind *E. coli*-Taspase1 at all recorded time points (~1 log concentration). Within the first 2 h only a minor fraction of CS2 was cleaved and about 75% remained uncleaved, even with up to 600 nM cfs-Taspase1 being present (equal to 600-fold molar excess of cfs-Taspase1: CS2). But after 24 h almost complete processing of CS2 was observed in samples containing cfs-Taspase1 in the 100 nM concentration range. This indicates that after purification from cfs the Taspase1 became activated within the first 24 h under the conditions of our assay. A concentration of 30 nM cfs-Taspase1 turned out to offer an optimal assay window. At this concentration barely any CS2 cleavage was observed after 2 h, but after 24 h about two-thirds of CS2 was cleaved, which caused a 3-fold reduction

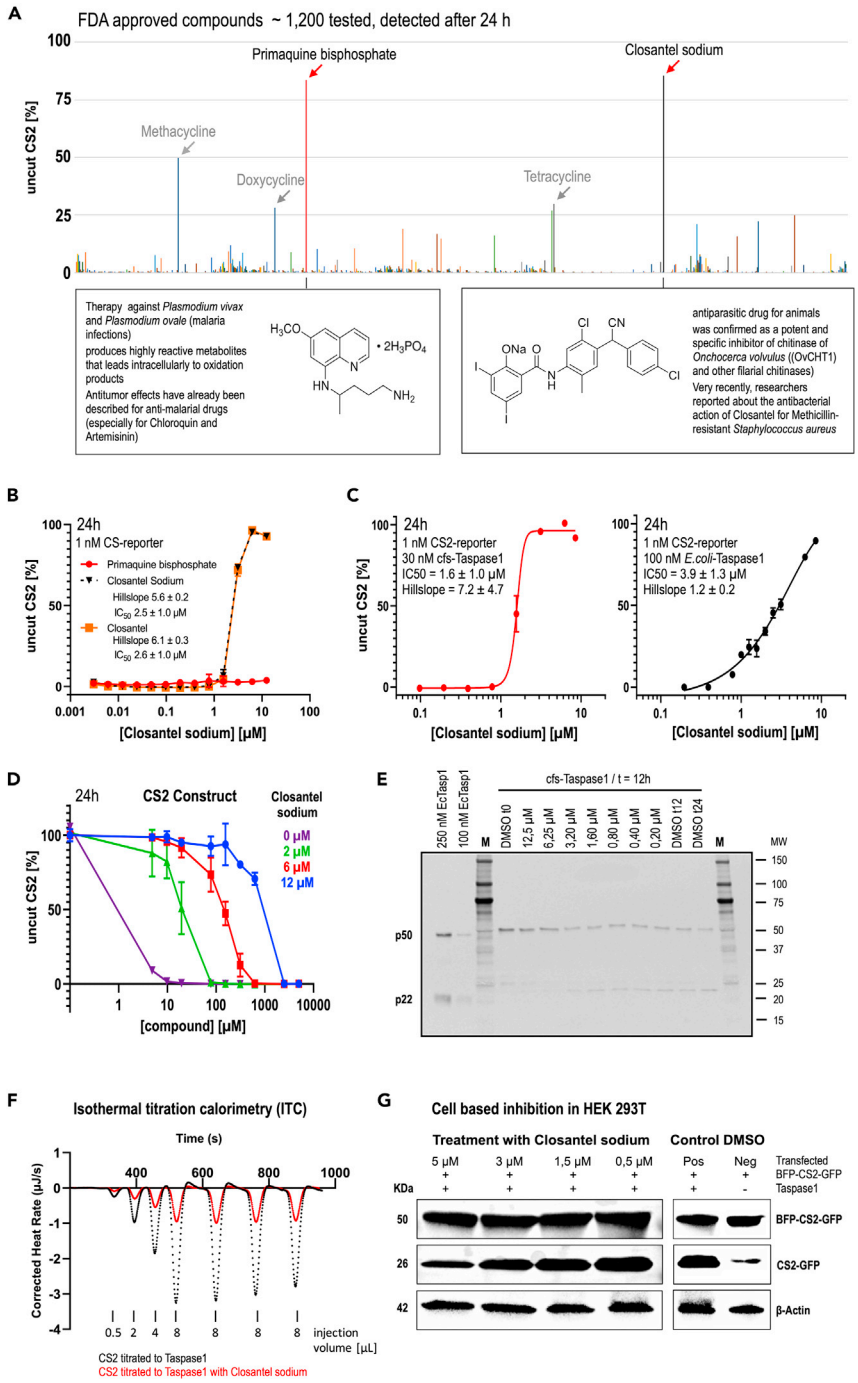

Figure 2. Screening potential inhibitors and validating candidate drugs

(A) Screening of FDA-approved drugs. The HTRF assay was used to screen a library with 1,200 FDA-approved drugs for their ability to inhibit cfs-Taspase1. The readout after 24 h incubation is presented; readout after 96 h is shown in Figure S1. About 25% uncut CS2 after 24 h was set as a threshold, and several candidates were identified. All identified Tetracycline derivatives were later identified as false positives showing autofluorescence in this assay. Two compounds were further investigated (Primaquine bisphosphate and Closantel sodium). Detailed information on both drugs is given below.

(B) HTRF CS2 cleavage assay as dose response for verification of the two initial hits. At concentrations up to 12.5 µM, Primaquine (red) did not prevent cleavage and was hence classified as false positive. Closantel with or without sodium as

Figure 2. *Continued*
counterion was validated as a novel potential Taspase1 inhibitor with an inhibitory activity in the low micromolar range. Data are the mean ± SD; n = 3.
(C) CS2 cleavage assay for verification of inhibition and estimation of IC_{50} for Closantel sodium acting on cfs- and *E. coli*-Taspase1. Substrate protein (1 nM) was incubated for 24 h with 30 nM cfs- or 100 nM of *E. coli*-Taspase1 protein, respectively. Data are the mean ± SD; n = 3. $R^2 \geq 0.986$. For cfs-Taspase1 the assay was performed in parallel also with 8 nM CS2 substrate protein of which cleavage was also detected using western blot as an orthogonal assay, which also served as a control for 0% uncut versus 100% uncut CS2 used for referencing (Figure S2). Analysis of the HTRF assay revealed that inhibition of cfs-Taspase1 by Closantel sodium is characterized by an even lower IC_{50} and a much steeper hill slope in comparison to the inhibition of *E. coli*-Taspase1.
(D) Same assay principle as employed in C, but instead of Closantel sodium here the *E. coli*-Taspase1 was titrated. CS2 substrate protein was set to 20 nM and treated for 24 h with Taspase1 ranging from 5 nM–5 μM or no Taspase1 as control. The inhibitory potential of Closantel sodium was tested at constant concentrations of 2, 6, and 12.5 μM with 5% DMSO in comparison to DMSO alone as control. Data are the mean ± SD; n = 4. After readout by HTRF, the corresponding quadruplicates were pooled, and cleavage of CS2 was detected by western blot; Figure S3.
(E) Cleavage assay of cfs-Taspase1 in the absence or presence of different concentrations of Closantel sodium. cfs-Taspase1 was freshly prepared, immediately transferred into HTRF assay buffer, and then incubated for 12 h at RT with Closantel sodium at the indicted concentrations or 5% DMSO alone. As references cfs-Taspase1 DMSO controls were also obtained at time point 0, 12, and 24 h. The two samples on the left show *E. coli*-Taspase1 for comparison. Activation of cfs-Taspase1 is not taking place when Closantel is present at a concentration >1.6 μM, which corresponds to the IC_{50} value determined in the HTRF assay.
(F) ITC experiments revealed that Closantel sodium is indeed attenuating the interaction between Taspase1 and CS2 substrate protein. CS2 (20 μM) was titrated into 1 μM *E. coli*-Taspase1 with or without 12.5 μM Closantel sodium being present. The baseline-corrected raw heat traces are presented as an overlay. Full evaluation is provided in Figure S5.
(G) Testing Closantel sodium in living cells. Closantel sodium is inhibiting the hydrolysis of a substrate protein (GFP-CS2-BFP) as detected by western blot. A reduction in the intensity of the 26 kDa protein band, which is corresponding to GFP-CS2, is indicative for the inhibitory capacity of Closantel on co-transfected Taspase1. β-Actin served as internal loading control.

in HTRF. This made the assay suitable for large-scale screening purposes within the first 24 h of *in vitro* Taspase1 production.

Screening experiments with different compound libraries revealed a single substance that is able to inhibit Taspase1

Using cfs-Taspase1, three libraries were screened in microplates. Two tested libraries gave no positive hits (100 small drugs, 100 fatty acids derivatives); however, when we screened a library composed of 1,200 FDA-approved drugs, we detected significant inhibition for several small molecules (see Figure 2A). After 24 h incubation time, some drugs displayed inhibitory effects. Inhibition of about 35% was observed for Doxycycline and Tetracycline; however, both substances exhibit substantial auto-fluorescence, which caused interference with the HTRF readout. This was even more pronounced with Methacycline (47% inhibition). Therefore, all three drugs were excluded from further studies. Two substances displayed an inhibition of Taspase1-mediated cleavage of CS2 substrate protein in the range of more than 80%; these 2 drugs were Primaquine bisphosphate and Closantel sodium.

Both substances were repurchased as dry stocks and dose-responses tested in the HTRF assay in order to verify the initial finding. As shown in Figure 2B, only Closantel either with or without sodium as counterion could be independently verified, whereas no inhibitory activity was detected for Primaquine bisphosphate. Therefore, only 1 candidate remained for further studies. All further experiments were conducted with Closantel sodium, which has a molecular weight of 685.1 Da.

IC_{50} estimations of Closantel sodium, a potential inhibitor for Taspase1

Next, we repeated the dose-response experiment in the HTRF CS2 cleavage assay in the protocol used for screening, and tested Closantel sodium in parallel against either cfs- or *E. coli*-Taspase1 (Figure 2C). Closantel sodium was tested in a range between 0 and 12.5 μM and inhibited both Taspase1 preparations with IC_{50} values of 1.6 μM on cfs- and 3.9 μM on *E.coli*-Taspase1, respectively. In order to exclude that observed inhibition by Closantel sodium could be an artifact, we also detected CS2 cleavage utilizing western blot (WB) as an orthogonal assay; Figure S2. The concentration of CS2 substrate was therefore slightly increased to 8 nM for optimal detection and treated with 30 nM cfs-Taspase1 in the presence of 0—12.5 μM Closantel sodium. The western blot fully validated the dose-dependent inhibition by Closantel sodium.

For cfs-Taspase1 a much steeper slope was observed in comparison to the experiment with *E. coli*-Taspase1 (Figure 2C). Such a steep slope is generally interpreted as an indication for a higher degree of cooperativity. In this case, it may indicate that Closantel sodium does not only inhibit the active Taspase1 but in addition prevents the maturation of the proenzyme into an active enzyme. Either a blockade of Taspase1 dimer formation and/or inhibition of auto-proteolytic cleavage within the dimer are in principle both possible modes of action that could explain the observed differences in the dose-dependent profiles of Closantel sodium. We then examined to what degree Closantel sodium is able to prevent cleavage of CS2. In order to determine the percentage of remaining uncleaved CS2, we switched back to the initial setup of the HTRF assay. *E. coli*-Taspase1 was titrated in presence of fixed concentrations of 2–6 to 12.5 μM Closantel sodium or DMSO as vehicle control. The concentration of CS2 was increased to 20 nM in order to allow for detection from the same samples in HTRF assay (Figure 2D) as well as in western blot (Figure S3). In agreement with previous experiments, 2 μM was not sufficient to completely prevent CS2 cleavage, whereas 12.5 μM Closantel sodium completely inhibited up to ~200 nM *E. coli*-Taspase1 for 24 h.

Mass-spectrometric experiments revealed no covalent binding of Closantel sodium

In order to understand the inhibitory effects in more details, we needed to clarify whether Closantel sodium had any effect on Taspase1 itself or the substrate protein. As shown in Figure S4, Closantel sodium did not covalently bind to Taspase1 nor to the CS2-substrate protein. The absence of irreversible binding was deduced from the unaltered mass of the proteins in the Closantel sodium treated versus DMSO control sample, respectively. These results demonstrated that Closantel sodium does not modify the substrate protein nor Taspase1 itself. Hence, Closantel sodium acts as a noncovalent inhibitor of Taspase1.

Investigation of cfs-Taspase1 in the presence of Closantel sodium

Next, we prepared cfs-Taspase1 and incubated it in HTRF assay buffer with DMSO or Closantel sodium at various concentrations (0.2 μM–12.5 μM). Samples were taken after 12 h and for reference additional DMSO controls also at time point 0 as well as after 12 and 24 h. Western blot was again employed to detect the 50 kDa and the 22 kDa bands corresponding to His-tagged Taspase1. As shown in Figure 2E, Closantel sodium inhibited the autoactivation of cfs-Taspase1 when the drug is applied at concentrations > the IC_{50} previously determined in the HTRF assay. Concentrations below 1.6 μM Closantel sodium allowed the activation of intrinsic serine protease function, which in turn leads to the cleavage of cfs-Taspase1 into its subunits (see p22 band arising). To this end, Closantel sodium is able to bind allosterically to Taspase1 subunits and may inhibit dimerization or allow dimerization but blocks the dimerization-induced movement of E296/S291 to perform the essential hydrolysis of the D233-T234 peptide bond in order to activate Taspase1.

ITC experiments demonstrated that Closantel sodium prevents Taspase1 from binding CS2

Next, we investigated the mode of action of Closantel sodium on already activated Taspase1. Isothermal titration calorimetry allows the measurement of the binding of a small molecule to a protein either directly or indirectly demonstrate its influence on complex formation between two proteins. Due to the limited solubility of Closantel sodium we opted for the latter. When *E. coli*-Taspase1 was titrated with CS2, an exothermic reaction was observed. As shown in Figure 2F, this was substantially reduced in presence of a constant concentration of 12.5 μM Closantel sodium. Full evaluation of individual ITC experiments showed that binding of CS2 to Taspase1 is in general rather weak as revealed by a constant enthalpy per mol of injectant across a large range of molar ratio; Figures S5A and S5B. This is in agreement with the time-dependent processing observed before in the HTRF assays. The presence of 12.5 μM Closantel sodium caused a substantial reduction of binding enthalpy per mol of injectant to about one-third. This indicates that Closantel sodium prevents Taspase1 from binding its substrate protein. From this experiment, we concluded that Taspase1, already intrinsically activated, is unable to bind to substrate protein. To this end, Closantel is not only able to inhibit dimerization/intrinsic activation but also prevented substrate binding.

Validation of Closantel sodium as a potential inhibitor of endogenous Taspase1

Finally, we investigated cleavage of a CS2-substrate in a cell-based experiment. HEK293T cells were transfected with plasmids for expression of a GFP-CS2-BFP, and Taspase1. The positive control showed cleavage (see 26 kDa GFP-CS2 cleaved protein fragment), whereas the negative control (only endogenous Taspase1 is active) showed a reduced 26 kDa band intensity. As shown in Figure 2G, treatment with Closantel

sodium resulted in a reduction of cleaved substrate protein. To this end, Closantel sodium can be used directly in cell culture experiments, as it enters the cells and inhibits Taspase1 at low micromolar concentrations.

DISCUSSION

Here we present the results of our efforts to identify a pharmacological inhibitor for Taspase1, a sequence-specific protease that has first been identified as a maturating enzyme of the MLL protein.

MLL protein family members contain the evolutionarily conserved Taspase1 recognition sites $Q^{-3}X^{-2}D^{-1}\bullet G^{1}X^{2}D^{3}D^{4}$. The human MLL protein exhibits CS1 (QVD•GADD) and CS2 (QLD•GVDD) that are localized at amino acid positions 2,666/2,667 and 2,718/2,719, respectively. Cleavage at CS2 is preferred over CS1, and thus, Taspase1-mediated hydrolysis of full-length MLL causes the generation of the described $p320^{N}$ and $p180^{C}$ MLL protein fragments (Hsieh et al., 2003a, 2003b) that assemble via the FYRN and FYRC domain into the MLL multiprotein complex (Pless et al., 2011). The fully assembled MLL multiprotein complex contains several other proteins (MEN1, LEDGF, CYP3, P3000, CBP, etc) and is important for reading and executing the histone H3 Lysine-4 trimethylations within promoter regions of actively transcribed genes.

Taspase1-dependent cleavage of MLL results in the destabilization of MLL, as part of a natural turn-over mechanism. Upon loss of Taspase1, MLL1 association with chromatin is markedly increased due to the stabilization of its unprocessed version, and this stabilization of the uncleaved MLL can result in the displacement of MLL chimeras (e.g., MLL-AF4) from chromatin in leukemic cells. Casein kinase II (CKII) phosphorylates MLL proximal to the Taspase1 cleavage site, facilitating its cleavage, and pharmacological inhibition of CKII blocks Taspase1-dependent MLL processing, increases MLL stability, and results in the displacement of the MLL chimeras from chromatin (Zhao et al., 2019).

Similarly, studies have revealed that TFIIA is also target of Taspase1-mediated cleavage (Dou et al., 2005): TFIIA consists of 3 subunits, TFIIAα (35 kDa), β (19 kDa), and γ (12 kDa). TFIIAα and β subunits are encoded by a single gene and result from site-specific cleavage of a 55 kDa TFIIA(α/β) precursor protein by the protease Taspase1. Metazoan cells have been shown to contain variable amounts of TFIIA (55/12 kDa) and Taspase1-processed TFIIA (35/19/12 kDa) depending on cell type (Malecová et al., 2015). TFIIA antagonizes negative TFIID regulators such as negative cofactor 2 (NC2), promotes specific binding of the TBP (TATA binding protein) subunit of TFIID to TATA core promoter sequence elements and stimulates the interaction of TBP-associated factors (TAFs) in the TFIID complex with core promoter elements located downstream of TATA, such as the initiator element (Inr). Taspase1 processing affects TFIIA regulation of TFIID, indicating that Taspase1 processing of TFIIA is required to establish INR-selective core promoter activity in the presence of NC2.

Recent publications drew attention to another hot topic: the role of TFIIA and its complex regulation—including the processing by Taspase1—and cranial-facial development during embryogenesis (Takeda et al., 2015). This included the first identification of a Taspase1 mutation (V343M) in a female with craniofacial anomalies, anterior segment dysgenesis, congenital immunodeficiency, and macrocytic anemia (Balkin et al., 2019), indicating the importance of the TFIIA downstream targets (e.g., Cdkn2a, p16Ink4a) during development.

Apart from these two major targets, overexpression of Taspase1 has been demonstrated in several cancers (Dong et al., 2014; Gribko et al., 2017; Zhang et al., 2020), which makes it an attractive target for development of a pharmacological inhibitor. However, because Taspase1 works in a stoichiometric rather than enzymatic fashion, this endeavor appears to be an impossible mission. Classical enzyme inhibition addresses either the catalytic center or functions in an allosteric fashion. For Taspase1, and the way in which this mono-enzymatic machinery becomes activated, the latter mode of action appears to be more promising, as so far any previous attempts to identify potential drugs that bind only the catalytic center have not yet identified a potential drug candidate that would allow further optimization (Lee et al., 2009; Chen et al., 2012; van den Boom et al., 2014).

Here we present the results of our efforts to identify potential inhibitors of Taspase1. Our assay strategy takes into account our knowledge of the molecular mechanism underlying Taspase1 activation (Sabiani et al., 2015). Based on these previous studies, dimerization of two Taspase1 monomers is a key event to activate the intrinsic serine protease function, which in turn activates the sequence-specific cleavage

mode of the Taspase1 dimer. Because Taspase1 cleaves its substrate in a stoichiometric fashion, any inhibitor that only addresses activated Taspase1 would likely only delay substrate cleavage. Whereas an inhibitor capable to prevent the interconnected dimerization and auto-catalytic maturation of Taspase1 would result in Taspase1 arrested in its inactive precursor form.

Therefore, we defined two important experimental prerequisites: (1) a sensitive assay system that allows monitoring of Taspase1 activity over 2–24 h (HTRF assay), as well as (2) the production of Taspase1 in a cell-free system for generation of a nonactivated "precursor" enzyme. We used two of our previously established Taspase1 mutants (see Figure 1A), e.g., the partially compromised V142A/L146A and the dominant-negative C163E/S291A double-mutants, to establish the HTRF assay. However, when screening for potential inhibitors, we used wild-type cfs-Taspase1 because these *in-vitro*-produced monomeric proteins need to dimerize and activate the intrinsic serine protease function in order to get an active Taspase1 dimer before CS2 cleavage can occur. Under the conditions applied, these consecutive processes are rather slow but are largely completed after 24 h. This allowed us to identify potential drugs that could potentially interfere with all these steps. In effect we could easily monitor inhibition of Taspase1 by comparison of HTRF readouts after 2 and 24 h.

We screened several libraries; however, the most promising one was the FDA-approved drugs library that resulted in the identification of Closantel sodium as a potential inhibitor. Closantel sodium is a salicylic acid anilide derivative that represents a well-known drug used for treatment of parasitic worm diseases in certain animals. Its pharmaceutical activity ranges from "liver flukes" (*Fasciola hepatica*) of hematotrophic nematodes to the "river blindness disease" (onchocerciasis) caused by the filarial worm Onchocerca volvulus. The precise mechanism of action is still unknown, but it likely has pleiotropic effects. Closantel sodium inhibits certain enzymes necessary for the life cycle of these parasitic nematodes (Garner et al., 2011; Gooyit et al., 2014), affects ion and liquid transport over membranes, uncouples the respiratory chain (ATP-production), and appears to possess some neurotoxic activity that selectively kills the parasitic organism (*Fasciola hepatica*, *Haemonchus contortus*, etc.). Closantel sodium is used for the treatment of cattle, sheep, and goats in a single dose ranging from 5 to 10 mg/kg body weight in cases of such parasitic infections. Moreover, Closantel sodium also exhibits antibiotic function, as it impacts on methicillin-resistant *Staphylococcus aureus* (Rajamuthiah et al., 2014).

Closantel sodium inhibited cleavage of the CS2 substrate protein with an IC_{50} between 1.6 and 3.9 μM, depending on which Taspase1 preparation we were using in our assay (cfs- or *E. coli*-produced). Based on the combined data presented in this manuscript, Closantel sodium does not covalently bind to either Taspase1 or CS2-substrate protein (Figure S4). Moreover, Closantel sodium clearly inhibited auto-activated Taspase1 but showed substantially higher potency on pre-mature Taspase1 (see Figures 2B–2E). Furthermore, only inhibition of the latter was characterized by a very steep slope, which indicates cooperativity and hence, some additional interconnected mechanism of inhibition that is only relevant on pre-mature Taspase1. Most likely, Closantel sodium prevents either dimerization or the small conformational changes (Sabiani et al., 2015) that are necessary for activating the intrinsic serine protease function that leads to the cleavage of the p50 Taspase1 into the active p28 and p22 Taspase1 subunits. Taking into account that pre-mature Taspase1 does not yet possess the active center of Taspase1, we conclude that Closantel sodium functions as an allosteric inhibitor rather than inhibiting the catalytic center of activated dimeric Taspase1. However, we cannot exclude that the potential binding site of Closantel sodium does also inflict with the N-terminal amino acid of the β-subunit (Thr234) that represent the catalytic center. All important amino acids (R262, E295, S291, Thr234) are very close in the published crystal structure of Taspase1 (Khan et al., 2005) or in the model presented by Sabiani et al. (2015) (Figure 6 therein).

Noteworthy, several experimental attempts of others in the past have also claimed to have identified Taspase1 inhibitors. But in these publications the authors used either extremely high concentrations of inhibitor 10–500 μM (Lee et al., 2009; Chen et al., 2012) or a CS2-peptidomimetic that could per definition only inhibit the catalytic center of an already activated Taspase1 dimer (van den Boom et al., 2014). In all cases, no one has ever found a substance that works in the low μM range and, moreover, inhibits the premature form of Taspase1 in an allosteric fashion.

Future work is necessary to explore this project further. We are currently trying to solve a high-resolution structure of Taspase1 in complex with Closantel sodium. This may unravel the mechanism of action and provide entrance points for rational drug design of more potent inhibitors.

Closantel sodium is already an approved drug, and hence, data on pharmacological characterization are readily available. Consequently, this novel inhibitor makes an optimal tool for further validation of Taspase1 as a target in leukemia or different solid cancers.

In summary, we present evidence that we have identified the first allosteric inhibitor of human Taspase1. This inhibitor will be helpful in future studies on diseases where Taspase1 has already been shown to be important. It may also foster future scientific efforts to understand this unusual, stoichiometrically working enzyme that has a very tight spectrum of known target proteins.

Limitations of the study

In order to study Taspase1 and its sequential maturation process, we made use of 2 different methods—at first, a commercial cell-free system for coupled *in vitro* transcription/translation in an *E. coli*-based extract (cfs-produced Taspase1) and second, the standard method of recombinant expression in *E. coli* (*E. coli*-produced Taspase1). Both methods have their pros and cons. Coupled *in vitro* transcription/translation is providing Taspase1 in limited amounts, however, mostly non-auto-activated, whereas *E. coli*-produced Taspase1 is mostly dimeric and therefore already auto-activated. However, *E. coli*-produced Taspase1 is available in much higher amounts. We have chosen primarily the coupled *in vitro* method, because we needed Taspase1 to undergo dimerization/auto-activation after being added to our assay system. This strategy opened up the opportunity to identify a drug that interferes with dimerization/auto-activation of Taspase1. By using only *E. coli*-produced Taspase1, we probably would have failed. What is still missing in the present study are subsequent experiments with this novel drug in different cancer cells. Such should be conducted in order to provide final evidence that Closantel is indeed preventing Taspase1 to hydrolyze its natural target proteins. Certain cancer entities with very high Taspase1 expression (pancreatic tumors, specific breast cancer subtypes) would be preferable model systems and could also provide additional insights into downstream effects. Finally, we have no animal model to study the identified drug in cancer, and hence, the present study does not provide any *in vivo* data.

QUANTIFICATION AND STATISTICAL ANALYSIS

Not applicable.

STAR★METHODS

Detailed methods are provided in the online version of this paper and include the following:

- KEY RESOURCES TABLE
- RESOURCE AVAILABILITY
  - Lead contact
  - Material availability
  - Data and code availability
- EXPERIMENTAL MODEL AND SUBJECT DETAILS
  - Animals
  - Cell culture
- METHOD DETAILS
  - Cloning of substrate protein
  - Plasmids for expression of Taspase1 wt and mutants
  - Protein expression in *E.coli* and purification
  - Cell-free expression of Taspase1
  - Labeling of SNAP fusion proteins with terbium cryptate
  - Generation of stable cell lines
  - In-cell CS2 cleavage assay in the presence of closantel sodium
  - Protein isolation from HEK293T cells
  - Western Blot
  - MALDI-TOF
  - Isothermal titration calorimetry

SUPPLEMENTAL INFORMATION

Supplemental information can be found online at https://doi.org/10.1016/j.isci.2021.103524.

ACKNOWLEDGMENTS

We are thankful for fruitful discussions within the cooperating labs. We thank Jakob Meier-Credo from the group of J.D.L. for mass spectrometry measurements. This work has been conducted and performed within the framework of the DFG grants MA 1876/12–1 and MA 1876/13-1.

AUTHOR CONTRIBUTIONS

Cloning, sequencing, acquisition of data, analysis, and interpretation of data (e.g., statistical analysis, biostatistics, computational analysis): VL, JH, EP. SK has given access to the FDA-based library for the screening experiment. Visualization of data, writing, and reviewing the original draft of the manuscript, project administration: JH and RM.

DECLARATION OF INTERESTS

The authors declare that they have no competing interests.

Received: August 2, 2021
Revised: November 11, 2021
Accepted: November 23, 2021
Published: December 17, 2021

REFERENCES

Balkin, D.M., Poranki, M., Forester, C.M., Dorsey, M.J., Slavotinek, A., and Pomerantz, J.H. (2019). TASP1 mutation in a female with craniofacial anomalies, anterior segment dysgenesis, congenital immunodeficiency and macrocytic anemia. Mol. Genet. Genomic Med. *7*, e818.

Brannigan, J.A., Dodson, G., Duggleby, H.J., Moody, P.C., Smith, J.L., Tomchick, D.R., and Murzin, A.G. (1995). A protein catalytic framework with an N-terminal nucleophile is capable of self-activation. Nature *378*, 416–419. https://doi.org/10.1038/378416a0.

Bursen, A., Moritz, S., Gaussmann, A., Moritz, S., Dingermann, T., and Marschalek, R. (2004). Interaction of AF4 wild-type and AF4•MLL fusion protein with SIAH proteins: indication for t(4;11) pathobiology? Oncogene *23*, 6237–6249.

Chen, D.Y., Liu, H., Takeda, S., Tu, H.C., Sasagawa, S., Van Tine, B.A., Lu, D., Cheng, E.H., and Hsieh, J.J. (2010). Taspase1 functions as a non-oncogene addiction protease that coordinates cancer cell proliferation and apoptosis. Cancer Res. *70*, 5358–5367.

Chen, D.Y., Lee, Y., Van Tine, B.A., Searleman, A.C., Westergard, T.D., Liu, H., Tu, H.C., Takeda, S., Dong, Y., Piwnica-Worms, D.R., et al. (2012). A pharmacologic inhibitor of the protease Taspase1 effectively inhibits breast and brain tumor growth. Cancer Res. *72*, 736–746.

Dong, Y., Van Tine, B.A., Oyama, T., Wang, P.I., Cheng, E.H., and Hsieh, J.J. (2014). Taspase1 cleaves MLL1 to activate cyclin E for HER2/neu breast tumorigenesis. Cell Res. *24*, 1354–1366.

Dou, Y., Milne, T.A., Tackett, A.J., Smith, E.R., Fukuda, A., Wysocka, J., Allis, C.D., Chait, B.T., Hess, J.L., and Roeder, R.G. (2005). Physical association and coordinate function of the H3 K4 methyltransferase MLL1 and the H4 K16 acetyltransferase MOF. Cell *121*, 873–885.

Garner, A.L., Gloeckner, C., Tricoche, N., Zakhari, J.S., Samje, M., Cho-Ngwa, F., Lustigman, S., and Janda, K.D. (2011). Design, synthesis, and biological activities of closantel analogues: structural promiscuity and its impact on Onchocerca volvulus. J. Med. Chem. *54*, 3963–3972.

Gooyit, M., Tricoche, N., Lustigman, S., and Janda, K.D. (2014). Dual protonophore-chitinase inhibitors dramatically affect O. volvulus molting. J. Med. Chem. *57*, 5792–5799.

Gribko, A., Hahlbrock, A., Strieth, S., Becker, S., Hagemann, J., Deichelbohrer, M., Hildebrandt, A., Habtemichael, N., and Wünsch, D. (2017). Disease-relevant signalling-pathways in head and neck cancer: taspase1's proteolytic activity fine-tunes TFIIA function. Sci. Rep. *7*, 14937.

Hartmann, M., Huber, J., Kramer, J.S., Heering, J., Pietsch, L., Stark, H., Odadzic, D., Bischoff, I., Fürst, R., Schröder, M., et al. (2021). Demonstrating Ligandability of the LC3A and LC3B adapter interface. J. Med. Chem. *64*, 3720–3746.

Hsieh, J.J., Cheng, E.H., and Korsmeyer, S.J. (2003a). Taspase1: a threonine aspartase required for cleavage of MLL and proper HOX gene expression. Cell *115*, 293–303.

Hsieh, J.J., Ernst, P., Erdjument-Bromage, H., Tempst, P., and Korsmeyer, S.J. (2003b). Proteolytic cleavage of MLL generates a complex of N- and C-terminal fragments that confers protein stability and subnuclear localization. Mol. Cell Biol. *23*, 186–194.

Khan, J.A., Dunn, B.M., and Tong, L. (2005). Crystal structure of human Taspase1, a crucial protease regulating the function of MLL. Structure *13*, 1443–1452.

Lee, J.T., Chen, D.Y., Yang, Z., Ramos, A.D., Hsieh, J.J., and Bogyo, M. (2009). Design, syntheses, and evaluation of Taspase1 inhibitors. Bioorg. Med. Chem. Lett. *19*, 5086–5090.

Malecová, B., Caputo, V.S., Lee, D.F., Hsieh, J.J., and Oelgeschläger, T. (2015). Taspase1 processing alters TFIIA cofactor properties in the regulation of TFIID. Transcription *6*, 21–32.

Marschalek, R. (2020). The reciprocal world of MLL fusions: a personal view. Biochim. Biophys. Acta Gene Regul. Mech. *1863*, 194547.

Mátés, L., Chuah, M.K., Belay, E., Jerchow, B., Manoj, N., Acosta-Sanchez, A., Grzela, D.P., Schmitt, A., Becker, K., Matrai, J., et al. (2009). Molecular evolution of a novel hyperactive sleeping beauty transposase enables robust stable gene transfer in vertebrates. Nat. Genet. *41*, 753–761.

Nagaratnam, N., Delker, S.L., Jernigan, R., Edwards, T.E., Snider, J., Thifault, D., Williams, D., Nannenga, B.L., Stofega, M., Sambucetti, L., et al. (2021). Structural insights into the function of the catalytically active human Taspase1. Structure *29*, 873–885.e5.

Nakamura, T., Mori, T., Tada, S., Krajewski, W., Rozovskaia, T., Wassell, R., Dubois, G., Mazo, A., Croce, C.M., and Canaani, E. (2002). ALL-1 is a histone methyltransferase that assembles a supercomplex of proteins involved in transcriptional regulation. Mol. Cell *10*, 1119–1128.

Niizuma, H., Searleman, A.C., Takeda, S., Armstrong, S.A., Park, C.Y., Cheng, E.H., and Hsieh, J.J. (2021). Taspase1 orchestrates fetal liver hematopoietic stem cell and vertebrae fates through cleaving TFIIA. JCI Insight *6*, e149382.

Oinonen, C., and Rouvinen, J. (2000). Structural comparison of Ntn-hydrolases. Protein Sci. *9*, 2329–2337. https://doi.org/10.1110/ps.9.12.2329.

Pédelacq, J.D., Cabantous, S., Tran, T., Terwilliger, T.C., and Waldo, G.S. (2006). Engineering and characterization of a superfolder green fluorescent protein. Nat. Biotechnol. *24*, 79–88.

Pless, B., Oehm, C., Knauer, S., Stauber, R.H., Dingermann, T., and Marschalek, R. (2011). The heterodimerization domains of MLL - FYRN and

FYRC - are potential target structures in t(4;11) leukemia. Leukemia *25*, 663–770.

Rajamuthiah, R., Fuchs, B.B., Jayamani, E., Kim, Y., Larkins-Ford, J., Conery, A., Ausubel, F.M., and Mylonakis, E. (2014). Whole animal automated platform for drug discovery against multi-drug resistant Staphylococcus aureus. PLoS One *9*, e89189.

Riddle, S.M., Vedvik, K.L., Hanson, G.T., and Vogel, K.W. (2006). Time-resolved fluorescence resonance energy transfer kinase assays using physiological protein substrates: applications of terbium-fluorescein and terbium-green fluorescent protein fluorescence resonance energy transfer pairs. Anal Biochem. *356*, 108–116.

Sabiani, S., Geppert, T., Engelbrecht, C., Kowarz, E., Schneider, G., and Marschalek, R. (2015). Unraveling the activation mechanism of Taspase1 which controls the oncogenic AF4-MLL fusion protein. EBioMedicine *2*, 386–395.

Takeda, S., Chen, D.Y., Westergard, T.D., Fisher, J.K., Rubens, J.A., Sasagawa, S., Kan, J.T., Korsmeyer, S.J., Cheng, E.H., and Hsieh, J.J. (2006). Proteolysis of MLL family proteins is essential for taspase1-orchestrated cell cycle progression. Genes Dev. *20*, 2397–2409.

Takeda, S., Sasagawa, S., Oyama, T., Searleman, A.C., Westergard, T.D., Cheng, E.H., and Hsieh, J.J. (2015). Taspase1-dependent TFIIA cleavage coordinates head morphogenesis by limiting Cdkn2a locus transcription. J. Clin. Invest. *125*, 1203–1214.

van den Boom, J., Mamić, M., Baccelliere, D., Zweerink, S., Kaschani, F., Knauer, S., Bayer, P., and Kaiser, M. (2014). Peptidyl succinimidyl peptides as taspase 1 inhibitors. Chembiochem *15*, 2233–2237.

Zhao, Z., Wang, L., Volk, A.G., Birch, N.W., Stoltz, K.L., Bartom, E.T., Marshall, S.A., Rendleman, E.J., Nestler, C.M., Shilati, J., et al. (2019). Regulation of MLL/COMPASS stability through its proteolytic cleavage by taspase1 as a possible approach for clinical therapy of leukemia. Genes Dev. *33*, 61–74.

Zhang, Y., Du, P., Li, Y., Zhu, Q., Song, X., Liu, S., Hao, J., Liu, L., Liu, F., Hu, Y., et al. (2020). TASP1 promotes Gallbladder cancer cell proliferation and metastasis by up-regulating FAM49B via PI3K/AKT pathway. Int. J. Biol. Sci. *16*, 739–751.

Zhou, H., Spicuglia, S., Hsieh, J.J., Mitsiou, D.J., Høiby, T., Veenstra, G.J., Korsmeyer, S.J., and Stunnenberg, H.G. (2006). Uncleaved TFIIA is a substrate for taspase 1 and active in transcription. Mol. Cell. Biol. *26*, 2728–2735.

STAR★METHODS

KEY RESOURCES TABLE

REAGENT or RESOURCE	SOURCE	IDENTIFIER
Antibodies		
Rabbit anti-GFP IgG, polyclonal antibody, unconjugated (1:1000; WB)	Abcam	Abcam Cat# ab290, RRID:AB_303395
Sheep anti-mouse IgG, monoclonal antibody, horseradish peroxidase conjugated (1:10,000; WB)	GE Healthcare	GE Healthcare Cat# NA931, RRID:AB_772210
Mouse anti-his-Tag (27 × 10^8), monoclonal antibody, unconjugated (1:1000)	Cell Signaling Technology	CST Cat# 2366, RRID:AB_2115719
Goat anti-Rabbit IgG, -horseradish peroxidase conjugated (1:10,000; WB)	Bio-Rad	Bio-Rad Cat# 170-6515, RRID:AB_11125142
Donkey anti-Rabbit IgG, conjugate with IRDye® 800CW (1:15,000; WB)	LI-COR	LI-COR Biosciences Cat# 926-32213, RRID:AB_621848
Bacterial and virus strains		
NEB® 5-alpha competent *E. coli*; DH5α™ derivative	NEB	NEB Cat# C2987
T7 express competent *E. coli*, BL21 DE3 derivative	NEB	NEB Cat# C2566
Chemicals, peptides, and recombinant proteins		
Q5® high-fidelity DNA polymerase	NEB	NEB Cat# M0491L
NEBuilder® HiFi DNA assembly master mix	NEB	NEB Cat# E2621L
KpnI-HF® restriction endonuclease	NEB	NEB Cat# R3142L
XhoI restriction endonuclease	NEB	NEB Cat# R0146L
T4 DNA ligase	NEB	NEB Cat# M0202S
SNAP-Lumi4-Tb labeling reagent; for labeling with terbium cryptate via SNAP-tag	cisbio	Cisbio Cat# SSNPTBD
Prestwick chemical Library®: FDA-approved & EMA-approved drugs for HTS screening	prestwick	Prestwick-chemical-library
Closantel sodium	Abcam	Abcam Cat# ab143384
Metafectene®	biontex	Biontex Cat# T020
EDTA-free cOmplete™ protease inhibitor cocktail tablets	Roche	Merck Cat# 11,697,498,001
Accutase cell detachment solution	Capricon	Capricon Cat# ACC-1B
Clarity max Western ECL substrate	Bio-Rad	Bio-Rad Cat# 1,705,062
2,5-Dihydroxybenzoic acid (DHB)	BRUKER	BRUKER Cat# 8,201,346
Experimental models: Cell lines		
HEK293T, human embryonic kidney 293 cells; derivative contains the SV40 T-antigen	ATCC	ATCC Cat# CRL-3216
Oligonucleotides		
494_sGFP_GSG_Stop.rev: 5′-CCCCCTCGAGTCTAA TCATTTAACCGGATCCTTTG TAGAGCTCATCCATGCCATGTG-3′	this paper	NA
495_TEVsite_SNAP_fusion.for: 5′-CCGACTACCGAAA ACCTGTACTTCCAGGGTACCG ACAAAGATTGCGAAATGAAACGTACCACCCTGG-3′	this paper	NA

(*Continued on next page*)

Continued

REAGENT or RESOURCE	SOURCE	IDENTIFIER
496_SNAP_CS2_fusion.rev: 5′-CATCAACACCATCCA ACTGTGAGATTTTCGGCAGA TCACCCAGACGATGACCTTCATGGGCCAG-3′	this paper	NA
497_CS2_sGFP.for: 5′-CTCACAGTTGGATGGTGTT GATGATGGTACGGAA TCCGCGAGCAAAGGAGAAGAACTTTTCACTGG-3′	this paper	NA
498_SNAP_CS1_fusion.rev: 5′-CAACACCATCCAAC TGTGAGATTTTCGGCAGATCA CCCAGACGATGACCTTCATGGGCCAG-3′	this paper	NA
499_CS1_sGFP.for: 5′-GGACAGGTGGATGGGGCC GATGACTTAAGCACT TCCGCGAGCAAAGGAGAAGAACTTTTCACTGG-3′	this paper	NA
594_MLL_D2718A.for: 5′-CAGTTGGCGGGTGTTGA TGATGGTACGGAATCCGCG-3′	this paper	NA
595_MLL_D2718A.rev: 5′-CAACACCCGCCAACTGT GAGATTTTCGGCAGATCACC-3′	this paper	NA
Recombinant DNA		
pSNAP-tag(T7)2; used as cloning template for SNAP-tag	NEB	NEB Cat# N9181S
pET29BH4	Hartmann et al. (2021)	NA
SNAP-CSx-sGFP in pET29BH4; used for expression of substrate proteins used in HTRF assay	This paper	NA
pRARE, a pACYC184 derived plasmid carrying tRNA genes for several codons rarely used in *E.coli*; plasmid was prepared from Rosetta™(DE3) competent cells - Novagen	Novagen	Merck Millipore Cat# 70,954-4
pET22b derived plasmids for expression of Taspase1 (wildtype and mutants) with C-term His_6-Tag	Sabiani et al. (2015)	NA
mTagBFP-CS2-mTagGFP2 (in pITR EZP vector); constitutively active promotor	Sabiani et al. (2015)	NA
Taspase1 (in pITR TCTH vector); Dox inducible expression	Sabiani et al. (2015)	NA
pCMV(CAT)T7-SB100	Mátés et al. (2009)	Addgene Cat# 34,879
Software and algorithms		
GraphPad PRISM, version 8; dose-response inhibition - log(inhibitor) vs. response with variable slope (four parameter fit)	GraphPad Software Inc.	Graphpad PRISM version 8
NanoAnalyze, data analysis program	TA instruments	NanoAnalyze version 3.10.0
Other		
Ni Sepharose® 6 fast flow	Cytiva	Sigma-Aldrich Cat# GE17-5318-02
Ultrafiltration membrane disc, ultarcel, PLGC, 10,000 MWCO	Merck	Merck Cat# PLGC04310
HiLoad® 16/600 Superdex® 75 pg	Cytiva	Sigma-Aldrich Cat# GE28-9893-33
HiLoad® 16/600 Superdex® 200 pg	Cytiva	Sigma-Aldrich Cat# GE28-9893-35
S30 T7 high-yield protein expression system	Promega	Promega Cat# L1110
His mag Sepharose® Ni beads	Cytiva	Sigma-Aldrich Cat# GE28-9673-90
PD spintrap G-25	Cytiva	VWR Cat# 28-9180-04
White non-treated polystyrene shallow well 384-well plates of the type Nunc™ 264,706	Thermo Fisher	ThermoFisher Cat# 264,706

(*Continued on next page*)

Continued

REAGENT or RESOURCE	SOURCE	IDENTIFIER
Tecan Infinite F200 pro	Tecan	NA
Tecan SPARK equipped with enhanced fluorescence module	Tecan	NA
4-20% Mini-Protean® TGXTM precast gels	Bio-Rad	Bio-Rad Cat# 4,561,096
Low fluorescence PVDF Western membrane	Abcam	Abcam Cat#
Precision plus Protein™ all blue standards; marker used for Western blots with fluorescence detection	Bio-Rad	Bio-Rad Cat# 1610373EDU
Odyssey nitrocellulose membrane; used for Western blots with fluorescence detection	Li-COR	Li-COR Cat# 926-31092
EveryBlot blocking buffer; used for Western blots with fluorescence detection	Bio-Rad	Bio-Rad Cat# 12,010,947
MALDI anchorchip targets	Bruker	Bruker Cat# 8,280,790

RESOURCE AVAILABILITY

Lead contact

Further information and requests for resources and reagents should be directed to and will be fulfilled by the lead contact, Rolf Marschalek (Rolf.marschalek@em.uni-frankfurt.de).

Material availability

All unique/stable reagents generated in this study are available from the lead contact with a completed Materials Transfer Agreement.

Data and code availability

All experimental data or any additional information required to reanalyze the data* reported in this paper are available from the lead contact.

EXPERIMENTAL MODEL AND SUBJECT DETAILS

Animals

Not applicable.

Cell culture

All work in mammalian cells has been carried out with HEK293T cells (ATCC CRL-3216) under sterile conditions. Cells were maintained in DMEM Low Glucose medium (DMEM-LPA, Capricorn Scientific) mixed with 10% (v/v) FBS (FBS-11A, Capricorn Scientific), and supplemented with 2 mM L-glutamine (STA-B, Capricorn Scientific), 100 U/mL penicillin and 100 µg/mL streptomycin (PS-B, Capricorn Scientific), and pre-heated to 37°C in a water bath before use. The cells were grown at 37°C in 5% CO_2 and a relative humidity of 95%. HEK293T cells were passaged every 3 days in order not to exceed a maximum confluence of ~80%. The old medium was removed using a vacuum pump, then the cells were washed with 5 mL PBS (PBS-1A, Capricorn Scientific) per 10 cm dish. After the PBS had been removed, the cells were detached with 1 mL Accutase (ACC-1B, Capricorn Scientific) per 10 cm cell culture plate and allowed to incubate at 37°C for 7-10 min. The cells were harvested and about 200 µL (1: 5) were sown on a new plate. The Accutase reaction was thereby stopped by the serum in the new medium (10 mL). After passaging, the cells should be about 20-30% confluent.

METHOD DETAILS

Cloning of substrate protein

The 20 kDa SNAP-tag (NEB) is a mutant of the DNA repair protein O^6-alkylguanine-DNA alkyltransferase. It reacts specifically with benzylguanine (BG) derivatives. Introduced mutations prevent completion of the enzymatic reaction which allows irreversible covalent labeling of SNAP fusion proteins. The HTRF based Taspase1 activity assay utilizes fusion proteins with N-terminal SNAP followed by a Taspase1 recognition

sequence, and C-terminal sGFP (superfolder green fluorescent protein) (Pédelacq et al., 2006). Plasmids for expression of such assay constructs were cloned based on the recently described pET29b derivative pET29BH4 (Hartmann et al., 2021) that encodes an open reading frame (ORF) for Met-Gly-[His_{10}-tag]-Asp-Tyr-Asp-Ile-Pro-Thr-Thr followed by a cleavage site for Tobacco Etch Virus protease [TEV site] and restriction sites for *KpnI* (in frame; first triplet is Gly codon of TEV site) and *XhoI*. The SNAP ORF (residues 2-177) was amplified by PCR using Q5 DNA polymerase (NEB), pSNAP-tag(T7)2 (NEB) as the template, and forward primer #495 in combination with either oligo #496 for attachment of CS2 or oligo #498 for attachment of CS1. In a second PCR the sequence for sGFP was amplified using as forward primer either #497 for CS2 or #499 for CS1 each in combination with reverse primer #494 that was used to attach the DNA sequence GGATCCGGT TAAATGATTAGA CTCGAG for Gly-Ser-Gly followed by stop codons in all reading frames, and *XhoI*. The forward primers for sGFP and the reverse primers for SNAP introduced (reverse complementary) overhangs that encode the Taspase1 recognition sequence to be cloned (either CS1 or CS2). After separate PCR reactions the products were fused by Gibson Assembly using NEBuilder HiFi DNA Assembly Master Mix (NEB), and cloned between *KpnI* and *XhoI* (NEB) using T4 DNA ligase, respectively. DH5α competent *E.coli* (NEB) were transformed, plasmids prepared using NucleoSpin Plasmid (Macherey-Nagel), and plasmids were verified by overlapping sequencing of the entire ORF. A mutant version of CS2 was generated by site directed mutagenesis using oligos #594 and #595.

The encoded ORFs read as follows; with amino acid sequence in single letter code, tags and proteins in brackets:

MG-[His_{10}]-DYDIPTT-[TEV site]-GT-[SNAP]-[Taspase1 recognition]-[sGFP]-GSG.

The Taspase1 recognition sequence is CS1 (KRSAEGQVDGADDLST), CS2 (DLPKISQLDGVDDGTE), or $CS2_{mut}$ (DLPKISQLAGVDDGTE), with the minimal heptamer underlined, respectively.

Plasmids for expression of Taspase1 wt and mutants

Cloning of Taspase1 wild type as well as mutants into pET22b (+) has previously been described (Sabiani et al., 2015). The plasmids code for full length Taspase1 followed by Leu-Glu and a C-terminal His_6-tag. For expression in the cell free system (cfs) we utilized the identical plasmid as for expression in *E.coli*.

Protein expression in *E.coli* and purification

Most of the proteins in this study were expressed in T7 Express (*E.coli* BL21 DE3 derivat, C2566, NEB) that carried the co-plasmid pRARE (Novagen). The proenzyme Taspase1 (wildtype Taspase1) in pET22b(+) and the construct SNAP-tag-CSx-sGFP in pET29BH4 were transformed in T7 Express + pRARE and cultured in liquid 100 mL LB medium (6673.4, Carl Roth) containing for Taspase1 in pET22b(+) 100 μg/mL Ampicillin (HP62.1, Carl Roth) or for SNAP-tag-CSx-sGFP in pET29BH4 35 μg/mL Kanamycin (T832.2, Carl Roth), and in either case 34 μg/mL Chloramphenicol (3886.2, Carl Roth) for pRARE. Cultures were grown at 37°C overnight at 180 rpm. For large scale protein production LB medium with appropriate antibiotics was inoculated with the transformed cells and shaken at 37°C until OD_{600nm} reached 0.8. At this point expression was induced with 0.5 mM IPTG (CN08.3, Carl Roth) and the temperature lowered to 20°C for overnight incubation at 20°C, shaking at 120 rpm. The next day, the cells were harvested by centrifugation for 10 min at 6000 rpm and 4°C. Afterward, the cell pellet was either stored at −80°C, or processed right away. For cell breakdown the cell pellets were resuspended in 50 mL lysis buffer (400 mM NaCl, 20 mM NaH_2PO_4 pH 7.8, 10% (w/v) glycerol and 20 mM β-mercaptoethanol) supplemented with 250 μL 5 M Imidazol, 750 Kunitz DNase I (D5025, Sigma-Aldrich), 250 Kunitz RNase A (R5503, Sigma-Aldrich), 2 mM $MgSO_4$, spatula tip of lysozyme form chicken egg white and 1× EDTA-free cOmplete protease inhibitor cocktail (11,697,498,001, Merck) and incubated for 30 min on ice. After incubation the suspension was passed 25 times with a pressure of 100 psi through an Invensys APV-1000 homogenizer (APV Systems, Silkeborg, Denmark). Cell debris was removed by centrifugation at 12,000 rpm for 15 min at 4°C.

The protein was purified by immobilized metal affinity chromatography (IMAC) using Ni Sepharose 6 Fast Flow (Cytiva) resin (on an ÄKTApurifier FPLC system (GE Healthcare) run with buffer A (400 mM NaCl, 20 mM NaPi pH 7,8, 10% (w/v) glycerol and 20 mM β-mercaptoethanol). The protein was washed with buffer B (buffer A with 25 mM imidazole) and eluted then with buffer C (buffer A with 300 mM imidazole). The fusion proteins with His_{10}-tag and TEV site were thereafter processed with His-tagged TEV protease in a dialysis setup against buffer A overnight at 4°C, thereby reducing imidazole to ~20 mM. The next day the protein

was run gravity flow through a column packed with the same Ni^{2+} resin to remove TEV protease and remaining uncleaved protein.

Thereafter, the flow through (SNAP fusion protein) or the elution from IMAC (Taspase1) was concentrated under 1.5 bar overpressure from nitrogen gas in an amicon stirring cell model 8050 (EMD Millipore) equipped with a 10.000 MWCO membrane disc (PLGC04310, Merck). The protein was then purified by size exclusion chromatography using a 16/600 Superdex75 (28-9893-33, Cytiva) for the assay constructs and for the Taspase1 a 16/600 Superdex200 column (28-9893-35, Cytiva). The column was equilibrated and run in HTRF buffer (25 mM HEPES pH 7.5, 150 mM KF, 10% (w/v) glycerol, 5 mM DTT) at 1 mL/min. The purity of the protein was monitored by SDS-PAGE. Clean fractions were pooled, flash frozen in liquid nitrogen, and stored at −80°C.

Cell-free expression of Taspase1

The *S30 T7 High-Yield Protein Expression System* (L1110, Promega) was used for cell-free protein expression. Based on this *E. coli* extract a desired protein can be expressed directly from a plasmid vector containing a T7 promotor and a properly positioned ribosome-binding site. In 1 h a yield of up to 500 μg/mL is possible to achieve. The protein expression was carried out according to the manufacturer's instructions as described in the technical manual. Protein expression was conducted for 1 h at room temperature (RT). Afterwards, the cell-free synthesis (cfs) reaction was supplemented per 50 μL with 1 μL RNase A (prepared according to the instructions in the manual; A7973 Promega) and in addition 1 μL DNase I (3000 Kunitz/mL in 20 mM Tris pH 8.0, 100 mM $MgSO_4$; D5025, SigmaAldrich). After 30 minutes at RT, purification was conducted using *His Mag Sepharose Ni-Beads* (28-9673-90, Cytiva) with buffer and volumes according to the manufacturer's instructions. The cfs-Taspase1 was finally eluted in His Mag buffer (20 mM NaH_2PO_4, 400 mM NaCl, 10% (w/v) glycerol) supplemented with 500 mM imidazole. For 450 μL cfs reaction 200 μL of a 50% slurry of *Ni-Beads* were used for purification that provides sufficient binding capacity for about 5 mg of His-tagged protein which made the initial yield from cfs expression the limiting factor. After elution cfs-Taspase1 concentration was reproducibly 600 nM ± 20%. For most assays the protein was diluted 1:20 in HTRF assay buffer resulting in a final concentration in the assay of 30 nM cfs-Taspase1.

For the assay presented in Figure 2E (inhibition of auto-activation) the imidazole from *His Mag* purification had to be removed as this assay was performed with undiluted cfs-Taspase1. Therefore, the cfs-Taspase1 was transferred into HTRF assay buffer (see HTRF assay for composition) using PD Spintrap G-25 (28-9180-04, Cytiva) salt exchange columns according to the manufacturer's instructions.

Labeling of SNAP fusion proteins with terbium cryptate

The protein constructs SNAP-tag-CS1-sGFP/SNAP-tag-CS2-sGFP/SNAP-tag-mut CS2-sGFP were labeled with SNAP-Lumi4-Tb (Terbium cryptate linked to SNAP pseudo substrate; SSNPTBD, Cisbio Bioassays, Codolet, France). The fluorophore was dissolved in dimethylsulfoxide (DMSO) to 100 μM. For labeling, 20 μL of the fluorophore (diluted to 10 μM in DMSO) were combined with 2 μL (120 μM) of the protein construct in 378 μL HTRF buffer (25 mM HEPES pH 7.5, 150 mM KF, 10% (w/v) glycerol, 5 mM DTT) and incubated at 4°C overnight. The labeled construct had an initial concentration of ~600 nM and was labeled theoretically to 80%. SNAP-tag as a coupling partner was used with a molar excess in order to prevent remaining free uncoupled fluorophore or cryptate. Labeled protein was stored at −20°C till use in the HTRF assay.

Homogeneous time-resolved fluorescence (HTRF) assay. The HTRF experiments were all performed in white non-treated polystyrene shallow well 384-well plates of the type Nunc 264,706 (264706, ThermoFisher) with a final assay volume of 20 μL/well. To avoid evaporation during incubation the plates were sealed with adhesive aluminum foil (4TI-0550; 4titude LTD, UK). In the HTRF assay, a buffer with optimized conditions for the proteins was used [25 mM HEPES pH 7.5, 150 mM KF, 5% (w/v) glycerol and freshly supplemented with 5 mM DTT, 5 mM $MgCl_2$, 0.1% (w/v) CHAPS]. Taspase1 (cfs- or *E.coli*-produced) at the indicated concentrations, CSx substrate protein at 1 nM (or 20 if indicated), and 5% (v/v) DMSO were combined. When testing a compound in dose-response the concentration of Taspase1 was set constant and the investigated compound was titrated instead. After pipetting all components into the plate, the reaction was incubated for 2 h or the indicated time at RT before fluorescence intensities (FI) at 520 nm (acceptor) and 620 nm (donor reference) each after excitation at 340 nm were recorded either on a Tecan Infinite F200 Pro or a Tecan SPARK (TECAN, Switzerland) equipped with enhanced fluorescence and filters

for all utilized wavelengths. Measurements were performed with 100 flashes, an integration time of 400 μs and a lag time of 100 μs. The gain was always set to optimal.

Calculation of the HTRF signal. According to convention FI_{520nm} was multiplied with 10,000 and divided by FI_{620nm} to obtain the dimensionless HTRF signal.

Library screen. 1,200 FDA-approved drugs (Prestwick Chemical Library), a custom designed library encompassing 100 kinase and protein-protein-interaction inhibitors (purchased from Enamine, provided by Prof Dr. Stefan Knapp) and 100 fatty acid derivatives (provided by Prof. Dr. Eugen Proschak) were used in this screen. All drugs in the library were dissolved in DMSO at a concentration of 10 μM. The compounds were initially tested at a concentration of 10 μM (1:1000 dilution) with 1 nM CS2 construct, freshly produced cfs-Taspase1 at a concentration of ~30 nM, and a final DMSO content of 5% in all wells. The positive control for this assay was the CS2 construct together with cfs-Taspase1, and as a negative control served the CS2 without Taspase1 each without compound but with 5% DMSO. All components were brought to room temperature before addition of CS2. Thereafter, fluorescence measurement was started immediately and was repeated once per hour for 24 h with a final read after 96 h. On the Tecan SPARK an HTRF read of an entire 384 plate took only about 15 minutes, and only half that per FI. This ensured minimal well-to-well offset. The humidity chamber of the Tecan SPARK was employed to prevent evaporation in between measurements. The negative and the positive control were used as reference for 100% and 0% uncut CS2. Hits were defined as drugs that have the ability to significantly inhibit the proteolytic cleavage of CS2 (≥25% uncut) as determined after 24 h. As the utilized cfs-Taspase1 had not yet gone through dimerization process and auto-proteolytic activation, observed inhibition could result either from interference with auto-activation of Taspase1 and/or from inhibition of active Taspase1. Hence, this assay setup is suited to identify compounds with various modes of action. Compounds that caused the fluorescence intensity of the donor to change by more than 25% were flagged as potential false positives.

Analysis of dose response. The dose-response study was performed to confirm identified hits from the primary screen and to determine the half-inhibitory concentration (IC_{50}). For confirmation of hits, Closantel sodium (Y0000392) and Primaquine bisphosphate (P2940000) were repurchased from Sigma-Aldrich and Closantel sodium from Abcam (ab143384), respectively. Stock solutions for dose response measurements were prepared in 100% DMSO, and serial dilutions were made immediately before each experiment. The reaction preparation and measurements were performed like in the library screen. Analysis of the dose response experiments was done using GraphPad PRISM, Version 8 (GraphPad Software Inc., USA) utilizing the dose-response inhibition - log(inhibitor) vs. response with variable slope (four parameters).

Generation of stable cell lines

Stable cell lines were generated using the Sleeping Beauty transposon system which enables stable integration of a specific DNA sequence (through ITR "internal tandem repeats") into the genome of a cell by means of a transposase. Transposition is a precise process in which a defined segment of DNA is cut out of a DNA molecule and inserted in another location in the same or within a different DNA molecule or genome. For the transfection of HEK293T cells, 4×10^6 with a confluency of 70% were sown onto a 10 cm tissue culture dish with 10 mL of medium, and grown for 24 hours. The medium was renewed 1 hour before the transfection. The transfection approach consisted of two components, solution A and solution B. Solution A was composed (for a 10 cm dish) of 180 μL PBS, 30 μL Metafectene (3× the μg DNA; T020, Biontex); solution B was composed of 180 μL PBS, 10 μg Sleeping Beauty vector DNA and 0.5 μg Transposase vector pCMV(CAT)T7-SB100 (Mátés et al., 2009). Solution B was slowly pipetted into solution A, resuspended and allowed to incubate for 15 min at room temperature. After the incubation, the mixture was evenly distributed and incubated for 24h. After 24h, the medium was changed and, depending on the viability of the cells and transfection efficiency, the cells were selected with the appropriate antibiotic (Puromycin 2 μg/mL; Hygromycin B 300 μg/mL, PUR-1X and HYG-H, Capricorn Scientific). The stable integration of the plasmids was monitored using the Observer Z1 fluorescence microscope from Carl Zeiss.

In-cell CS2 cleavage assay in the presence of closantel sodium

Cells were stably transfected with the construct mTagBFP-CS2-mTagGFP2 (in pITR EZP vector) and Taspase1 (pITR TCTH vector; Sabiani et al., 2015). 10^6 cells in 10 mL medium were placed in a 10 cm culture dish and left for 24 hours at 37°C in an atmosphere of 5% CO_2. The next day, medium was replaced and

the cells were treated with Closantel sodium (diluted in DMSO) at final concentrations of 0.5, 1.5, 3, 5 μM and 1% DMSO or DMSO alone as negative control. At the same time expression of Taspase1 was induced by addition of 1 μg/mL doxycycline. Cells were then incubated for 48 h at 37°C with 5% CO_2. Cells that only expressed the CS2 substrate construct were used as negative control.

Protein isolation from HEK293T cells

For the production of cell lysates, the cells were first washed with PBS followed by treatment with 1 mL Accutase (ACC-1B, Capricon) for a 10 cm culture dish at 37°C for about 10 minutes. The cells were transferred to 1.5 mL reaction vessels and centrifuged for 5 min at 1,000 rpm. After separating the supernatant from the pellet, the pellet was resuspended in 500 μL lysis buffer (150 mM NaCl, 10 mM Tris-HCl (pH 7,4), 1 mM EDTA, 1 mM EGTA (pH 8), 1% Triton-X100 und 0.5% NP-40) and freshly given 1× EDTA-free cOmplete protease inhibitor cocktail (11697498001, Merck) and allowed to rotate at 4°C for 30 min. The lysate was then centrifugated at 14,000 rpm at 4°C for 60 min. The supernatant was transferred to a new 1.5 mL reaction vessel and frozen at −20°C.

Western Blot

Proteins were separated on 4-20% Mini-Protean TGX Precast gels (4561096, Bio-Rad) for 45 min at 250 V. Transfer to PVDF membranes (Low Fluorescence Western Membrane, ab133411, Abcam) was carried out using the semi-dry process. Using the Trans-Blot TURBO from Bio-Rad, the proteins were transferred using a standard transfer program (25 V, 0.4 A, 30 min for 2 midi gels). The membrane was blocked with 5% BSA in TBS buffer containing 1 mL Tween 20 per liter (hereafter named 0.1% TBS-T) for 1h at RT. After that the membrane was washed 3 times with 0.1% TBS-T. Then a specific antibody was added and allowed to rotate overnight at 4°C and 20 rpm in presence of 5% BSA in 0.1% TBS-T. The next day, the membrane was washed again 3 times with 0.1% TBS-T, then incubated with a secondary HRP-conjugated antibody for 1 h at room temperature under the same conditions as used for the primary antibody, and finally washed again with 0.1% TBS-T. The proteins were detected using the Clarity Western ECL Blotting Substrate System (1705062, Bio-Rad) and the visualization was carried out on a Molecular Imager Chemi DOC XRS + from Bio-Rad. For the experiments shown in Figures 2C and 2D in parallel cleavage of CS2, or inhibition thereof, was shown also by Western blot in parallel experiments which are documented in Figures S2 and S3. Rabbit anti-GFP IgG (ab290; Abcam) and mouse α-His-Tag IgG1 (2366; Cell Signaling Technology) were used as primary antibodies for GFP (Figure 2G) or His-tag, respectively. Anti-Mouse IgG (NA931, GE Healthcare) and goat anti-Rabbit IgG (170-6515, Bio-Rad) were used as secondary antibody accordingly.

For the experiment shown in Figure 2E the Western blot protocol was changed to fluorescence detection on a Li-COR Odyssey 9120. Therefore, Precision Plus Protein All Blue (1610373EDU, Bio-Rad) was used as marker and Odyssey nitrocellulose membranes (926-31092, Li-COR) were used instead of PVDF, but using the same transfer protocol. The membrane was blocked in EveryBlot Blocking buffer (EBB; 12010947; Bio-Rad) for 1 h at RT, followed by overnight incubation with primary antibody anti-His-Tag (1:1000 in EBB; 2365, Cell Signaling Technology) at 4°C. Then the membrane was washed 3 times with 0.1% TBS-T before incubation with IRDye 800CW Donkey anti-Rabbit IgG (926-32213, Li-COR) as secondary antibody (1:15000 in EBB) for 1 h at RT. The membrane was again washed 3 times with 0.1% TBS-T followed by one additional wash in TBS without Tween.

MALDI-TOF

MALDI-MS measurements were conducted on a Bruker Rapiflex mass spectrometer (linear positive mode) using a MALDI Anchorchip target (8280790, Bruker) and DHB (2,5-Dihydroxybenzoic acid) matrix with (1:1 mixture of protein and matrix, DHB 300mg/mL in 1:1 H2O:Acetonitrile with 0.1% TFA (Trifluoroacetic acid); standard dried droplet sample preparation). All solvents were LC-MS grade and purchased from Thermo (H2O #047146.K2, Acetonitrile #047138.K2), DHB matrix was purchased from Bruker (8201346, Bruker). At first Taspase1 (45 μM in 250 μL, à 512 μg, MW 45581 Da) was measured. Next, the combination of Taspase1 (9 μM, 105.5 μg) incubated for 1 h with Closantel sodium (450 μM, 77 μg, 686.9 Da) was analyzed. In second set of experiments the CS2 construct (45 μM in 250 μL, à 535 μg, MW 47539 Da) alone, and the combination CS2 construct (9 μM, à 106.9 μg, MW 47539 Da) with Closantel sodium (450 μM, 77 μg, 686.9 Da) were analyzed.

Isothermal titration calorimetry

ITC experiments were performed at 25°C using an "Affinity ITC" (TA-Instruments) equipped with a 174 µL cell. *E.coli*-Taspase1 and the SNAP-CS2-sGFP protein were used. ITC measurements were conducted in 25 mM HEPES, 150 mM KF, 5 mM DTT, $5\%_{(w/v)}$ glycerol, pH 7.8 supplemented with 5% DMSO, 5 mM $MgCl_2$ and $0.1\%_{(w/v)}$ CHAPS. The samples were centrifuged for 10 min at 14.000 rpm and then degassed for 30 min. Due to the limited solubility of Closantel sodium its effect had to be determined indirectly as a modulation of the interaction between Taspase1 and CS2 substrate protein. CS2 (20 µM) was then titrated into 1 µM Taspase1 with or without 12.5 µM Closantel sodium being present. The titrations were carried out using 7 injections of 0.5 µL, 2 µL, 4 µL, 4 × 8 µL and a time interval between injections of at first 60 and later 120 seconds. For the control experiments, the cell contained only buffer or buffer with Closantel, respectively. The data analysis program NanoAnalyze (version 3.10.0, TA Instruments) was used for evaluation. Data were baseline-corrected and integrated before controls were subtracted by individual injection.